

Transport, magnetic, and structural properties of spinel MnTi_2O_4 and the effect of V doping

T. Sonehara,¹ K. Kato,^{2,3} K. Osaka,² M. Takata,^{2,3} and T. Katsufuji^{1,4}

¹*Department of Physics, Waseda University, Tokyo 169-8555, Japan*

²*JASRI/SPring-8, Hyogo 679-5198, Japan*

³*CREST, Japan Science and Technology Corporation, Saitama 332-0012, Japan*

⁴*PRESTO, Japan Science and Technology Corporation, Saitama 332-0012, Japan*

(Received 3 April 2006; revised manuscript received 15 August 2006; published 29 September 2006)

We studied the transport, magnetic, and structural properties of spinel MnTi_2O_4 and V-doped samples, $\text{MnTi}_{2-x}\text{V}_x\text{O}_4$, to clarify the relation between charge, spin, and orbital degrees of freedom of $3d$ electrons in this series of compounds. A structural phase transition occurs in MnTi_2O_4 at 180 K, which is presumably dominated by the ordering of t_{2g} orbitals, but it can be easily suppressed by the V doping to the Ti site. Associated with this suppression of the structural anomaly, a ferrimagnetic and electrically conducting state appears in $\text{MnTi}_{2-x}\text{V}_x\text{O}_4$ with finite values of x . Fairly large magnetoresistance was observed in this state, whose sign changes from positive to negative with an increase in the V concentration x . With approaching the other end of this series, MnV_2O_4 , the electrical resistivity increases again and another type of structural phase transition occurs at 53 K. Large magnetostriction was observed in MnV_2O_4 , the only compound in this series to have both a ferrimagnetic state and tetragonal lattice distortion.

DOI: [10.1103/PhysRevB.74.104424](https://doi.org/10.1103/PhysRevB.74.104424)

PACS number(s): 75.47.-m, 75.80.+q, 75.50.Gg, 61.10.-i

I. INTRODUCTION

In spinel oxides (AB_2O_4), there are two cations (A and B) in the ratio of 1:2. Cation A is surrounded by four oxygen ions, forming isolated AO_4 tetrahedra, whereas cation B is surrounded by six oxygen ions, forming edge-sharing BO_6 octahedra. When the B sites are occupied by transition metals, the t_{2g} states of the d orbital (triply degenerate d_{xy} , d_{yz} , and d_{zx}) between neighboring B sites have a larger interaction than the e_g states (doubly degenerate d_{z^2} and $d_{x^2-y^2}$) because of the geometrical configuration of the B and O sites (edge-sharing BO_6 octahedra). This large interaction as well as threefold degeneracy of the t_{2g} states leads to intriguing phenomena in spinel oxides with early transition metals (Ti, V). For example, ZnV_2O_4 (Refs. 1–3) with V^{3+} ($3d^2$) is a Mott insulator and exhibits a structural transition at 60 K and antiferromagnetic ordering at 40 K, which are correlated with each other. MgTi_2O_4 (Refs. 4 and 5) with Ti^{3+} ($3d^1$) also exhibits a structural transition at 250 K and shows an insulating behavior at low temperatures. It was proposed^{6–8} that these structural anomalies in spinel oxides with early transition metals are caused by the ordering of t_{2g} orbitals, which are coupled with the spin degree of freedom of $3d$ electrons by the so-called Kugel-Khomskii interaction.⁹

Though the spin degree of freedom plays an important role for these phenomena in early-transition-metal spinel oxides, most of them are not sensitive to external magnetic field. This is because magnetic susceptibility of the compounds above is suppressed owing to the strong antiferromagnetic coupling between B-site spins. We recently proposed¹⁰ that to put magnetic Mn^{2+} ions ($3d^5$, $S=5/2$) on the A site (tetrahedral site) of the spinel structure is a promising way to enhance magnetic susceptibility and to have a large magnetic-field effect. For example, MnV_2O_4 , which can be regarded as the Mn^{2+} -substituted compound for the Zn^{2+} site of ZnV_2O_4 , shows a magnetic-field switching of the crystal structure (i.e., orbital states), which arises from the

enhanced magnetic-field effect through the Mn-V coupling.

The aim of the present work is to apply this idea to other spinel oxides with early transition metals. Here, we choose MgTi_2O_4 and substituted nonmagnetic Mg^{2+} by magnetic Mn^{2+} . As mentioned above, MgTi_2O_4 with Ti^{3+} ($3d^1$) exhibits a structural transition from a cubic to tetragonal phase at 250 K. Recent x-ray and neutron diffraction measurement⁵ revealed that Ti-Ti dimers are formed in a helix pattern in the tetragonal phase of MgTi_2O_4 , and this Ti-Ti dimer is in a spin-singlet state composed of two $3d^1$ states, resulting in a sharp drop of magnetic susceptibility at 250 K. The first issue to be addressed here is what happens to this Ti-Ti dimerization when nonmagnetic Mg^{2+} is substituted by magnetic Mn^{2+} and magnetic interaction between Mn^{2+} and Ti^{3+} is introduced. In addition, this introduction of magnetic Mn^{2+} ions allows another channel of the external magnetic field to couple with Ti spins via the Mn-Ti interaction, and a larger magnetic-field effect in its consequence is expected.

In the present work, we also study the mixed compounds between MnTi_2O_4 and MnV_2O_4 , i.e., $\text{MnTi}_{2-x}\text{V}_x\text{O}_4$. MnV_2O_4 has V^{3+} ions ($3d^2$) and is known to exhibit a structural phase transition at 53 K.^{11,12} Since the orbital degree of freedom plays an important role also for MnV_2O_4 ,¹⁰ it can be expected that the mixture of Ti and V yields different characteristic behaviors arising from the cooperation of two different orbital-active ions. Indeed, we observed electrically conducting behaviors in $\text{MnTi}_{2-x}\text{V}_x\text{O}_4$ around $x=1$, and large negative magnetoresistance.

It should be stressed that the transport, magnetic, and structural properties of MnTi_2O_4 and V-doped compounds are dominated by charge, spin, and orbital degrees of freedom of $3d$ electrons, respectively. In the present study, a particular focus is on the correlation between these three degrees of freedom. For example, magnetoresistance and magnetostriction are the phenomena arising from the cooperation of the spin and charge, or the spin and orbital degrees of freedom, and their measurement provides us with important information on the issue.

II. SAMPLE PREPARATION AND EXPERIMENT

Polycrystalline samples of MnTi_2O_4 as well as V-doped samples, $\text{MnTi}_{2-x}\text{V}_x\text{O}_4$ ($0 \leq x \leq 2$), were synthesized by solid-state reaction in a sealed quartz tube. Appropriate amounts of Mn_3O_4 , TiO_2 , Ti , and V_2O_3 with the nominal composition $\text{MnTi}_{2-x}\text{V}_x\text{O}_{3.9}$ were mixed, ground, pressed into pellets, sealed under vacuum in a quartz tube, and sintered at 1100°C . We measured x-ray diffraction by a laboratory x-ray source to check the sample quality, as well as to obtain the cubic lattice constants at room temperature. It was found that an impurity phase of colundum structure (probably Mn doped Ti_2O_3) always exists in MnTi_2O_4 , and its amount becomes minimum when the nominal oxygen number is 3.9 in our sintering condition. The amount of the impurity is reduced with V doping, and no impurity phase was observed for $\text{MnTi}_{2-x}\text{V}_x\text{O}_4$ with $x \geq 1.2$. Since both colundum Ti_2O_3 and ilumenite MnTiO_3 are insulators with small magnetic susceptibility, the existence of the impurity phase does not largely affect the discussion below. The cubic lattice constant of $\text{MnTi}_{2-x}\text{V}_x\text{O}_4$ varies almost linearly with x from $x=0$, MnTi_2O_4 (8.63 Å), to $x=2$, MnV_2O_4 (8.52 Å).

Resistivity measurement was done by a conventional four-probe method with silver paste as electrodes. Lattice striction was measured by a strain-gauge technique. Both resistivity and striction measurements were also done under magnetic field with a 5 T superconducting magnet. Magnetization was measured by a superconducting quantum-interference-device (SQUID) magnetometer.

Synchrotron x-ray diffraction measurement was carried out at SPring-8 BL02B2 equipped with a large Debye-Sherrer camera.¹³ Polycrystalline samples were crushed into powder, and then a precipitation method was applied to get fine powder with a homogeneous size. The powder was sealed in a 0.3 mm ϕ quartz capillary, and temperature was controlled by a low-temperature (90–300 K) N_2 gas flow system. The wavelength of the x-ray was 0.7515 Å.

III. RESULTS

A. Properties of MnTi_2O_4

Figure 1(a) is an Arrhenius plot of the temperature (T) dependence of resistivity (ρ) for MnTi_2O_4 . $\log \rho$ linearly increases with $1/T$, and the activation energy at low T is estimated as 0.072 eV. As shown by the arrow, there is an anomaly in $\rho(T)$ around 180 K. The derivative of $\log \rho(T)$ is also plotted in the inset to show the anomaly more clearly. This increase of $\rho(T)$ is analogous to the anomaly in $\rho(T)$ of MgTi_2O_4 at 250 K,⁴ where a structural transition from a cubic to tetragonal phase occurs.

To see if there is a similar structural anomaly in MnTi_2O_4 , we measured the striction ($\Delta L/L$) as a function of T by a strain-gauge technique. As can be seen in Fig. 1(b), $\Delta L/L$ shows an abrupt decrease around 180 K, which is the same T as that of the $\rho(T)$ anomaly. These results indicate that a structural anomaly occurs also in MnTi_2O_4 at $T_c=180$ K.

To study the detailed crystal structure of MnTi_2O_4 , synchrotron powder x-ray diffraction was measured at low temperatures. Though clear splitting of the fundamental peaks

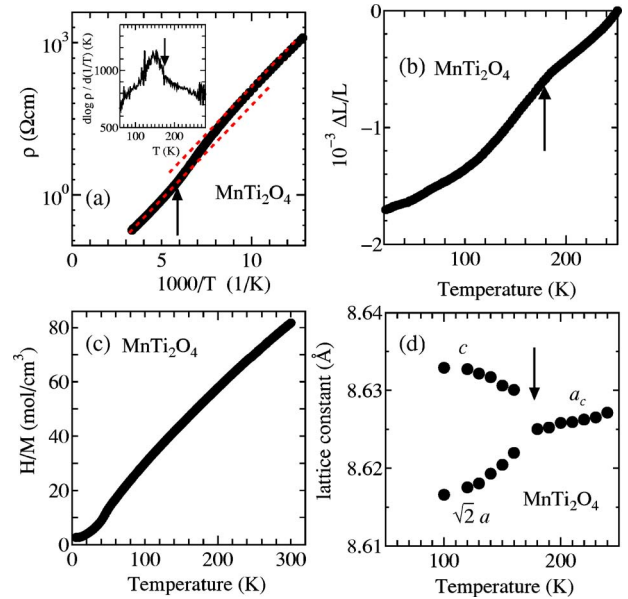


FIG. 1. (Color online) (a) Arrhenius plot of resistivity (ρ) and $\log \rho$ differentiated by inverse temperature $1/T$ (inset). Temperature dependence of (b) striction, (c) inverse magnetization, and (d) lattice constants obtained by synchrotron x-ray diffraction, for MnTi_2O_4 . The arrows refer to a structural phase transition. Since the primitive cell of the tetragonal phase (below 180 K) becomes $a_c/\sqrt{2} \times a_c/\sqrt{2} \times a_c$ of the cubic phase (above 180 K), c and $\sqrt{2}a$ are plotted in the tetragonal phase in (d).

was barely observed even at 100 K ($<T_c$), anisotropic broadening of several Bragg peaks was observed, as shown in Fig. 2. Among them, the (400) and the (440) peak do show broadening, but the (111) peak does not. In addition, the

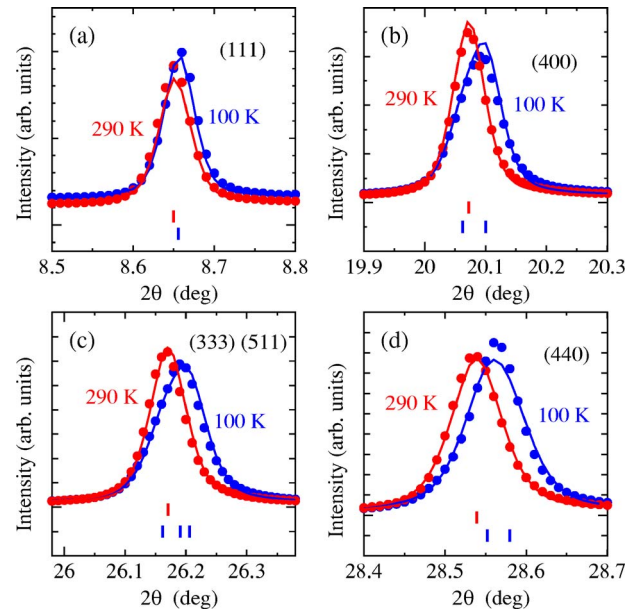


FIG. 2. (Color online) Synchrotron x-ray powder diffraction patterns (closed circles), Rietveld refinement patterns (solid lines), and the position of Bragg peaks (vertical marks) of MnTi_2O_4 at 290 and 100 K around the (a) (111); (b) (400); (c) (333), (511); and (d) (440) peaks.

TABLE I. Atomic parameters of MnTi_2O_4 at 290 K [$Fd\bar{3}m$, $a=8.62956(9)$ Å] and 100 K [$I4_1/amd$, $a=6.09303(9)$ Å, $c=8.6331(1)$ Å] from synchrotron x-ray powder diffraction refinements. $R_{\text{wp}}=9.32$ and $R_c=2.06$ for the 290 K data, and $R_{\text{wp}}=9.49$ and $R_c=1.93$ for the 100 K data.

| Atom | Site | x | y | z | B (Å ²) |
|---------------------------|------|-----------|--------------|-----------|--------------------------|
| <hr/> | | | | | |
| MnTi_2O_4 | | 290 K | $Fd\bar{3}m$ | | |
| Mn | 8a | 0 | 0 | 0 | 0.45(2) |
| Ti | 16d | 0.625 | 0.625 | 0.625 | 0.47(1) |
| O | 32e | 0.3874(1) | 0.3874(1) | 0.3874(1) | 0.82(4) |
| <hr/> | | | | | |
| MnTi_2O_4 | | 100 K | $I4_1/amd$ | | |
| Mn | 4a | 0 | 0.75 | 0.125 | 0.28(2) |
| Ti | 8d | 0 | 0 | 0.5 | 0.30(1) |
| O | 16h | 0 | 0.0191(6) | 0.2693(5) | 0.26(4) |

anisotropic broadening of the (400) peak is such that a tail appears on the lower angle. These results suggest that the low T phase is tetragonal with $c > a$. We made a Rietveld analysis of the data with a space group $I4_1/amd$, a simple elongation of cubic spinel ($Fd\bar{3}m$) along the c axis, and the lattice constants obtained by the analysis are shown in Fig. 1(d). Here, the primitive cell of the tetragonal phase becomes $a_c/\sqrt{2} \times a_c/\sqrt{2} \times a_c$ of the cubic phase, and the a lattice constant multiplied by $\sqrt{2}$ and the c lattice constant are plotted in the tetragonal phase. Below 180 K, the difference between $\sqrt{2}a$ and c gradually increases with decreasing T . The atomic parameters of MnTi_2O_4 at 290 K (cubic phase) and 100 K (tetragonal phase) are summarized in Table. I. It should be pointed out that, though the c axis is longer than $\sqrt{2}a$ in the tetragonal phase of MnTi_2O_4 , the Ti-O octahedral are compressed along the c axis, and the Ti-O distance becomes 1.99 Å for the apical oxygen and 2.08 Å for the in-plane oxygen at 100 K.

This structural phase transition at 180 K is analogous to that of MgTi_2O_4 at 250 K,^{4,5} but there are several differences between these two compounds. One is that the c lattice constant is shorter than the $\sqrt{2}a$ in the tetragonal phase of MgTi_2O_4 , but is longer in the present MnTi_2O_4 . Second, the difference between $\sqrt{2}a$ and c amounts to $\sim 0.5\%$ in MgTi_2O_4 but only $\sim 0.15\%$ in MnTi_2O_4 . This smaller distortion of the crystal structure might be responsible for the smaller jump of $\rho(T)$ at the transition temperature in MnTi_2O_4 . Finally, the superlattice peaks appearing in the tetragonal phase of MgTi_2O_4 as a result of the Ti-Ti dimerization (and the disappearance of the body-centered symmetry) are barely observed in MnTi_2O_4 in the synchrotron x-ray powder diffraction. We discuss the possible origin of this structural anomaly at 180 K in Sec. IV.

The inverse magnetic susceptibility [$1/\chi(T)$] of MnTi_2O_4 is shown in Fig. 1(c). As can be seen, $1/\chi(T)$ is linear, and its extrapolation intersects with the x axis almost at $T=0$, i.e., Curie-paramagnetic behavior. The Curie constant estimated

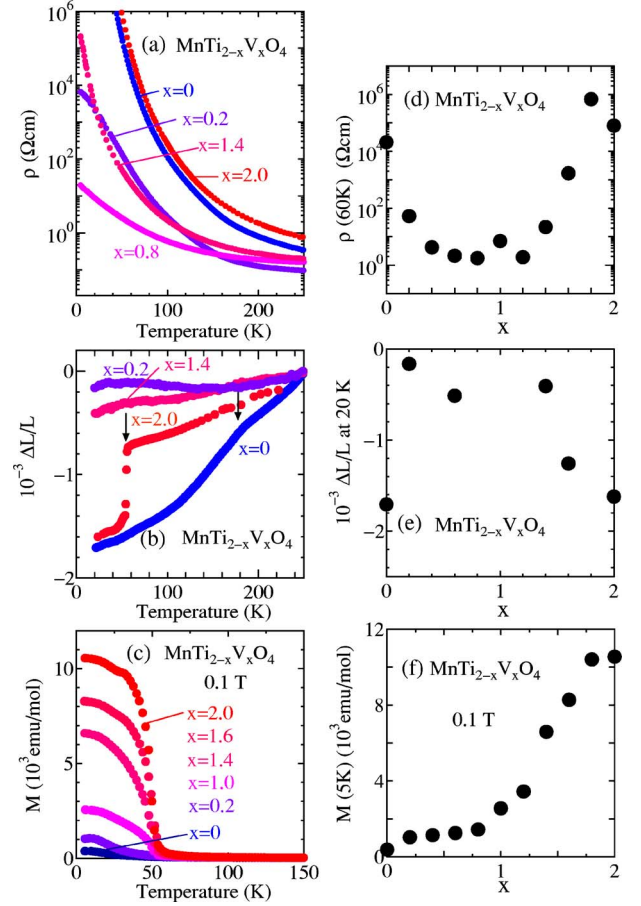


FIG. 3. (Color online) Left: Temperature dependence of (a) resistivity, (b) striction, and (c) magnetization of $\text{MnTi}_{2-x}\text{V}_x\text{O}_4$ at various values of x . The arrows in (b) refer to structural phase transitions. Right: x dependence of (d) resistivity at 60 K, (e) striction at 20 K, and (f) magnetization at 5 K.

from the slope of $1/\chi(T)$ is consistent with the $S=5/2$ spin on each Mn^{2+} site. These results indicate that the Mn spins are barely interacting with each other in MnTi_2O_4 . For MgTi_2O_4 , a drop of $\chi(T)$ at $T_c=250$ K was observed,⁴ corresponding to a spin-singlet formation associated with the Ti-Ti dimerization, but that kind of anomaly is barely observed in MnTi_2O_4 . Note that the drop of $\chi(T)$ ($\sim 1 \times 10^{-4}$) can be easily masked, even if it exists, by the presence of a large Curie term in MnTi_2O_4 ($\sim 2 \times 10^{-2}$ at 180 K). Thus, the direct evidence of the singlet formation of Ti spins in the present MnTi_2O_4 has yet to be obtained.

B. Properties of $\text{MnTi}_{2-x}\text{V}_x\text{O}_4$

The temperature dependence of resistivity [$\rho(T)$] of $\text{MnTi}_{2-x}\text{V}_x\text{O}_4$ at various values of x is shown in Fig. 3(a). For $x=0$ (MnTi_2O_4), $\rho(T)$ diverges at low temperatures, as discussed above. On the other hand, $\rho(T)$ also diverges at low temperatures for $x=2.0$ (MnV_2O_4), indicating that MnV_2O_4 is a Mott insulator. A conspicuous aspect of the $\rho(T)$ data is that the ρ value at low T is substantially suppressed in the mixed compounds around $x=1$, as summarized

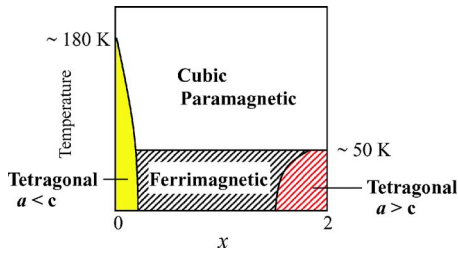


FIG. 4. (Color online) Schematic phase diagram of $\text{MnTi}_{2-x}\text{V}_x\text{O}_4$. The shaded area corresponds to the ferrimagnetic phase.

in Fig. 3(d). For the most conducting samples, $\rho(T)$ at the lowest T is suppressed to $\sim 10^1 \Omega \text{ cm}$, though $\rho(T)$ still increases with decreasing T , which might arise from the disorder of the conduction band composed of the mixture of Ti and V $3d$ states. We noted that a similar conducting state in the mixture of Ti^{3+} and V^{3+} has been observed in $\text{MgTi}_{2-x}\text{V}_x\text{O}_4$ (Ref. 14) and $\text{LaTi}_{1-x}\text{V}_x\text{O}_3$.¹⁵

The temperature dependence of striction exhibits a similar variation with x in $\text{MgTi}_{2-x}\text{V}_x\text{O}_4$ [Figs. 3(b) and 3(e)]. For $x=0$ (MnTi_2O_4), there is an anomaly of $\Delta L/L$ at 180 K, as discussed above. On the other hand, there is an anomaly of $\Delta L/L$ at 53 K for $x=2.0$ (MnV_2O_4), corresponding to a structural phase transition into a tetragonal phase.¹¹ This structural phase transition of MnV_2O_4 is different from that of MnTi_2O_4 at 180 K in that (i) the c lattice constant is shorter than $\sqrt{2}a$ in MnV_2O_4 ,^{10,11} (ii) resistivity is already insulating above the transition temperature in MnV_2O_4 , and (iii) the structural phase transition is correlated with a ferrimagnetic ordering in MnV_2O_4 .¹⁰ These anomalies, however, disappear in the mixed compound $\text{MgTi}_{2-x}\text{V}_x\text{O}_4$ for $0 < x < 2.0$, where $\Delta L/L$ exhibits only a monotonic temperature dependence. This is quite analogous to the behaviors of electrical resistivity shown in Figs. 3(a) and 3(d), where only the mixed compounds exhibit a conducting behavior.

The temperature dependence of magnetization [$M(T)$] of $\text{MnTi}_{2-x}\text{V}_x\text{O}_4$ under 0.1 T is shown in Fig. 3(c). For $x=0$ (MnTi_2O_4), there is almost no anomaly in $M(T)$, as discussed above. On the other hand, for $x=2.0$ (MnV_2O_4), there is an increase of $M(T)$ below 56 K, corresponding to a ferrimagnetic state, where the Mn and V spins align to the opposite direction.¹¹ As can be seen, $M(T)$ below 50 K increases also for the mixed compounds, $\text{MnTi}_{2-x}\text{V}_x\text{O}_4$ [see also Fig. 3(f)]. It is reasonable to assign this increase of $M(T)$ for $0 < x < 2.0$ also to the same type of the ferrimagnetic state as that of MnV_2O_4 . This means that a ferrimagnetic state appears with V doping to MnTi_2O_4 . The results of magnetic and structural properties in $\text{MnTi}_{2-x}\text{V}_x\text{O}_4$ are summarized in Fig. 4 as a schematic phase diagram of x vs temperature.

Here, it should be pointed out that most of the spinel oxides (AB_2O_4) with two transition metals on the A and B site become a ferrimagnet (irrespective of the existence of a structural phase transition), which arises from the antiferromagnetic A-B interaction. Thus, MnTi_2O_4 , where the ferrimagnetic state is absent, is quite unique, and its mechanism

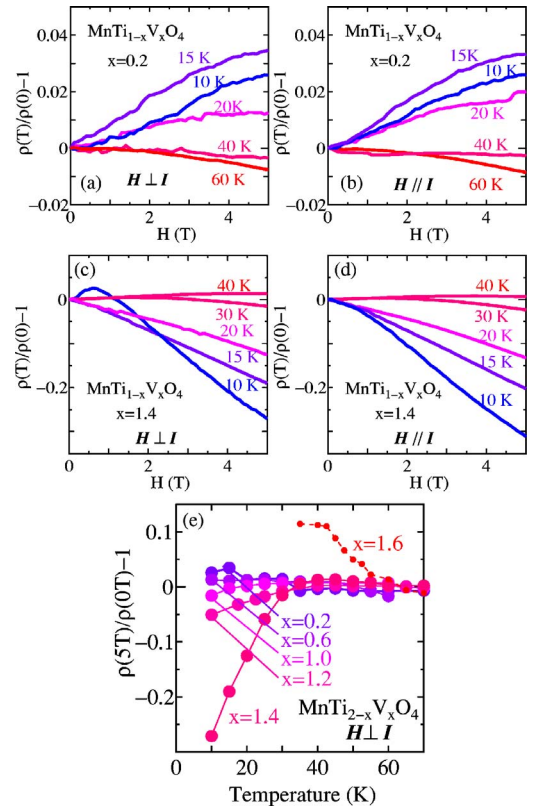


FIG. 5. (Color online) (a)–(d) Magnetic-field dependence of resistivity. Magnetic field was applied perpendicular to the electric-current direction (left) as well as parallel to it (right). (e) Magnitude of magnetoresistance at 5 T as a function of T at various values of x .

needs to be clarified. A possible key is the experimental results above that the absence of the ferrimagnetic state in MnTi_2O_4 and its appearance with V doping seem to be correlated with the existence of a structural anomaly in MnTi_2O_4 and its disappearance with V doping, as well as the insulating behavior of MnTi_2O_4 and a conducting behavior with V doping. This issue will be discussed in Sec. IV.

C. Magnetoresistance and magnetostriction in $\text{MnTi}_{2-x}\text{V}_x\text{O}_4$

The magnetic-field dependences of resistivity (magnetoresistance), $\rho(H)$, for $\text{MnTi}_{2-x}\text{V}_x\text{O}_4$ with $x=0.2$ and $x=1.4$ are shown in Figs. 5(a)–5(d). For both samples, the magnetoresistance data with $I \parallel H$ and $I \perp H$ (I is the electric current and H the magnetic field) are plotted. As can be seen, ρ for $x=0.2$ increases with increasing H (positive magnetoresistance) both with $I \parallel H$ and $I \perp H$ below 30 K, whereas ρ for $x=1.4$ decreases with increasing H (negative magnetoresistance) both with $I \parallel H$ and $I \perp H$ below 30 K. The magnitude of magnetoresistance at 5 T [$\rho(5T)/\rho(0T)-1$] is plotted as a function of T at various values of x in Fig. 5(e). There are several characteristics in this magnetoresistance: (i) almost isotropic against the direction of the magnetic field, (ii) its absolute value increases with decreasing T , (iii) its sign at low T continuously changes from positive to negative with increasing x . This continuous change of the sign of magne-

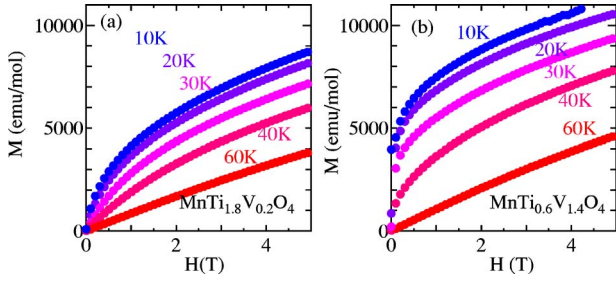


FIG. 6. (Color online) Magnetic field dependence of magnetization at various temperatures for $\text{MnTi}_{2-x}\text{V}_x\text{O}_4$ with (a) $x=0.2$ and (b) $x=1.4$.

toresistance with the variation of composition is characteristic of this series of compounds, and barely observed in other transition-metal oxides. A careful observation of Figs. 5(a)–5(d) leads to another characteristic, (iv) the sign changes also with T around 40 K, above which magnetoresistance becomes positive for large x , and negative for small x . Positive magnetoresistance above 40 K in the large x region is more clearly seen for $x=1.6$ in Fig. 5(e), though we could not measure the magnetoresistance of this sample below 40 K because its resistivity diverges for that T range.

To understand the second point (the increase of magnetoresistance at low T), M - H curves were measured for $x=0.2$ and $x=1.4$ at various temperatures [Figs. 6(a) and 6(b)]. For $x=1.4$, there is spontaneous magnetization (M at $H \sim 0$) below 40 K, corresponding to the ferrimagnetic ordering, but the magnitude of magnetization (M) keeps on increasing with further applied magnetic field even at the lowest temperature. Previous neutron scattering measurement on MnV_2O_4 indicates that its ferrimagnetic state is such that V spins are canted from the opposite direction of the Mn spin (the so-called triangular magnetic structure).¹¹ Therefore, the change of the canting angle might be the origin of the increase of M with further applied magnetic field in the ferrimagnetic phase of $\text{MnTi}_{2-x}\text{V}_x\text{O}_4$. We speculate that this variation of the magnetic state by magnetic field is responsible for the magnetoresistance at $T \ll T_N$. It is to be noted that the behavior at finite H for $x=0.2$ is almost the same as that for $x=1.4$, though the spontaneous magnetization is much smaller.

Magnetostriction was also studied for $\text{MnTi}_{2-x}\text{V}_x\text{O}_4$. It was reported that MnV_2O_4 ($x=2.0$) shows large magnetostriction below T_N , which is anisotropic against the direction of the magnetic field.¹⁰ The magnetic field dependence of striction in MnV_2O_4 below $T_N=56$ K is shown in Fig. 7(d). As can be seen, the crystal structure is contracted along the magnetic-field direction, whereas elongated perpendicular to it, and the absolute value of striction amounts to $\Delta L/L \sim 10^{-3}$. On the other hand, for $\text{MnTi}_{2-x}\text{V}_x\text{O}_4$ with $x=1.4$ [Fig. 7(c)], anisotropy of magnetostriction against the direction of magnetic field is the same as that of MnV_2O_4 , but its absolute value ($\Delta L/L \sim 10^{-4}$) is one order of magnitude smaller than that of MnV_2O_4 . Magnetostriction is barely observed in $\text{MnTi}_{2-x}\text{V}_x\text{O}_4$ with $x=0.2$ and $x=0$ (MnTi_2O_4). These results can be summarized that large magnetostriction in this series of compounds is characteristic of the tetragonal phase with spontaneous magnetization, i.e., MnV_2O_4 .

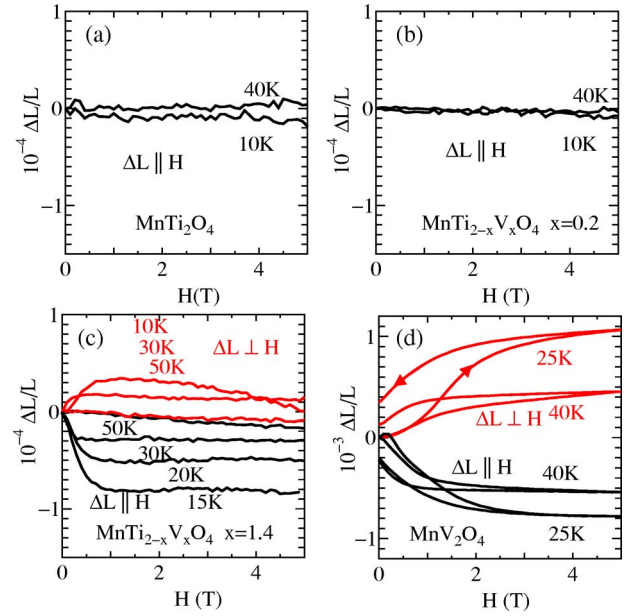


FIG. 7. (Color online) Magnetic-field dependence of striction for $\text{MnTi}_{2-x}\text{V}_x\text{O}_4$ with (a) $x=0$, (b) $x=0.2$, (c) $x=1.4$, and (d) $x=2$. Note that the scale is ten times different for (d) MnV_2O_4 .

IV. DISCUSSION

A. Origin of the anomaly at 180 K in MnTi_2O_4

First, let us discuss the origin of the structural anomaly in MnTi_2O_4 . Regarding the structural phase transition and the Ti-Ti dimerization in MgTi_2O_4 , Khomskii and Mizokawa⁸ proposed an “orbital-driven Peierls” model, where the “tetramerization” of t_{2g} orbitals, like $d_{zx}-d_{zx}-d_{yz}-d_{yz}$ ordering along a certain Ti chain (in the [011] or [101] directions, but not in the [110]) is the origin of the structural phase transition and spin-singlet formation. Though it is reasonable to attribute the structural anomaly of MnTi_2O_4 also to the ordering of Ti 3d orbitals, we could not find any superlattice peak in the low-temperature tetragonal phase. Thus, a possibility is that there is a ferro-orbital ordering below 180 K, where all d electrons occupy the same t_{2g} state. Since the TiO_6 octahedra are compressed along the c axis, the nondegenerate xy state is split from the doubly degenerate yz and zx states to lower energy, and it is likely that the Ti electrons are occupying the nondegenerate xy state below 180 K.

Unlike the case of MgTi_2O_4 , where the Ti spins form singlet pairs, the Ti spins survive even in the tetragonal phase with the orbital state above. To explain the absence of the ferrimagnetic state in MnTi_2O_4 , therefore, we have to assume that the Mn-Ti interaction is not strong enough to overcome the Mn-Mn antiferromagnetic interaction. Note that the Mn spins with antiferromagnetic interaction with each other on the tetrahedral site of the spinel structure is subject to the frustration arising from the geometry of the lattice (diamond lattice). The ferrimagnetic state in the V-doped samples can be explained by assuming that the Mn-V interaction is stronger than the Mn-Ti interaction and enough to overcome the Mn-Mn interaction. The insulating behavior of MnTi_2O_4 and the conducting behavior of the V-doped samples can be pos-

sibly explained by the ordering and the melting of the Ti t_{2g} orbitals.

There are several issues, however, that cannot be explained by the scenario above. For example, the crystal structure is elongated along the c axis, though the TiO_6 is compressed along the c axis, and there is no reason to be so in the ferro-orbital state. Instead, this implies that there is a formation of the Ti-Ti bond along the ab plane. Since the crystal is contracted along the ab plane in MnTi_2O_4 , one possibility is that the same type of the spin-singlet orbital Peierls state exists in the present MnTi_2O_4 , but along the $[110]$ direction. We should also point out that powder x-ray diffraction cannot detect the peaks with intensity weaker than 10^{-4} times that of the fundamental peaks. Indeed, the intensity of superlattice peaks in many charge-ordered compounds (manganites and nickelate with the K_2NiF_4 structure, for example) is so weak so that they cannot be detected by powder diffraction measurement. Thus, the absence of the superlattice peaks in the present powder x-ray diffraction does not necessarily exclude the possibility of their existence,

This Ti-Ti bond scenario can explain the magnetic properties naturally. For MnTi_2O_4 , the Mn-Ti interaction, which is essential for the ferrimagnetic state, does not work since all the Ti spins form spin-singlet pairs and there is no spin on the B site. When V is doped to the Ti site and the Ti-Ti dimerization is suppressed, the A-B antiferromagnetic interaction becomes effective and yields a ferrimagnetic state, consistent with the experimental result. Since the spontaneous magnetic moment in the intermediate range of x is smaller than $1\mu_B$ per $\text{Mn}(\text{Ti},\text{V})_2\text{O}_4$ mole, which is the minimum value of the spontaneous magnetic moment in the ideal ferrimagnetic state of $\text{MnTi}_{2-x}\text{V}_x\text{O}_4$, the Mn spins are not fully polarized in this x range, presumably owing to the Ti-Ti dimerization locally surviving in $\text{MnTi}_{2-x}\text{V}_x\text{O}_4$.

It is critical to this scenario whether the superlattice peaks arising from the Ti-Ti bond formation in the $[110]$ direction exist or not in MnTi_2O_4 , and the experiment should be done in the future, preferably using a single crystal.

B. Origins of magnetoresistance and magnetostriction

Let us discuss the possible mechanism of magnetoresistance for the present compounds. One of the typical mechanisms of magnetoresistance in magnetic conductors is a double-exchange mechanism, seen in perovskite manganites, which arises from the Hund coupling between localized spins and itinerant carriers. However, this mechanism only produces negative magnetoresistance, inconsistent with the behaviors of the present compounds. Also, many mechanisms of magnetoresistance, including the double-exchange mechanism, predict the enhancement of magnetoresistance around a spin-ordering temperature, which is not observed in the present compound.

To explain the positive magnetoresistance of $\text{MnTi}_{2-x}\text{V}_x\text{O}_4$ for the small x region, the Zeeman shift of the exchange-split bands, which is recently proposed as the mechanism of the positive magnetoresistance in $(\text{Fe},\text{Co})\text{Si}$,¹⁶ is the most likely mechanism. $\text{MnTi}_{2-x}\text{V}_x\text{O}_4$ around $x=1$ is conducting and has a conduction band, which we speculate is

formed of the Ti/V $3d$ states and the oxygen $2p$ states with a large amount of disorder. In the ferrimagnetic phase, there are the majority and minority spin bands for the conduction bands. The splitting between the majority and minority spin bands is further increased associated with the applied magnetic field and the increase of magnetization (Zeeman shift). Since electrical resistivity is dominated by the scattering rate (τ), the effective mass (m^*), and the Fermi velocity (v_F) of both the majority and minority spin bands, the change of the splitting between these two bands and a change of the position of the Fermi energy in each band result in the change of resistivity, either in the increasing or decreasing direction (and increasing direction in this case).

We point out that when the ferrimagnetic moment is evolved for the larger x region, where the smaller V spins ($S=1$) align to the opposite direction of the larger Mn spins ($S=5/2$), applied magnetic field leads to the decrease of the spontaneous V moment, and the splitting of the majority and minority spin bands also decreases in its consequence. This gives the opposite effect to the magnetoresistance (negative magnetoresistance), even though the band parameters and the scattering rate is the same. Therefore, one possible scenario is that for the smaller x region, where the ferrimagnetic moment is only partially evolved, applied magnetic field leads to the increase of the polarization of the V spins and further splitting of the majority and minority spin bands. However, for the larger x region, where the ferrimagnetic moment is already evolved, the situation is totally opposite and this difference results in the sign change of magnetoresistance with x . This scenario naturally explains the positive magnetoresistance above 40 K for the large x region, since the ferrimagnetic moment is not fully evolved and it is likely that the V spins align more with applied magnetic field in this T range.

Finally, let us discuss the mechanism of magnetostriction in $\text{MnTi}_{2-x}\text{V}_x\text{O}_4$. According to the experimental result, large magnetoresistance in this series of compounds is characteristic of the tetragonal phase with spontaneous magnetization. This indicates that large magnetostriction of MnV_2O_4 can be attributed to the change of tetragonal-domain directions with applied magnetic field, which is caused by the preferred orientation of the magnetic moment against the direction of the tetragonal domain. Since the c axis is shorter in the tetragonal phase of MnV_2O_4 , it can be concluded that the magnetic moment is preferably oriented along the c axis in this compound.

V. SUMMARY

We have investigated transport, magnetic, and structural properties, which are dominated by charge, spin, and orbital degrees of freedom of $3d$ electrons, respectively, for spinel $\text{MnTi}_{2-x}\text{V}_x\text{O}_4$. We found that $\rho(T)$ of MnTi_2O_4 shows an anomaly around 180 K associated with the structural transition, and $\text{MnTi}_{2-x}\text{V}_x\text{O}_4$ shows a conducting behavior around $x=1.0$ associated with the disappearance of the structural anomaly. We also found that there is no ferrimagnetic state in MnTi_2O_4 , whereas $\text{MnTi}_{2-x}\text{V}_x\text{O}_4$ with finite values of x becomes a ferrimagnet associated with the disappearance of the

structural anomaly. A possible scenario for these behaviors is that ordering of the Ti t_{2g} orbitals, either ferro- or antiferro-ordering, occurs at 180 K in MnTi_2O_4 and that dominates the transport and magnetic properties of this series of compounds.

We also found magnetoresistance, which is positive ($x < 1.0$), negative ($x \geq 1.0$) at the lowest T , and isotropic against the direction of magnetic field. A possible explanation for this unique magnetoresistance is the Zeeman shift of the exchange split bands, and the opposite response of the V spins to magnetic field associated with the evolution of the ferrimagnetic state. Finally, we found large magnetostriction, which is anisotropic against the direction of the magnetic field, in the sample of the tetragonal phase with spontaneous magnetization, i.e., MnV_2O_4 . This indicates that the reorien-

tation of tetragonal domains associated with the direction of the spontaneous magnetization is the origin of large magnetostriction in MnV_2O_4 .

ACKNOWLEDGMENTS

We thank T. Suzuki and K. Adachi for their help in the early stage of the study, and T. Mizokawa and D. I. Khomskii for fruitful discussions. This work was partly supported by Grants-in-Aid for the 21st Century COE Program at Waseda University, "Academic Frontier" Project, and for Young Scientists (A), from MEXT of Japan. The synchrotron radiation experiments were performed at the BL02B2 in the SPring-8 with the approval of the Japan Synchrotron Radiation Research Institute (JASRI) (Proposal No. 2005B0092).

-
- ¹Y. Ueda, N. Fujiwara, and H. Yasuoka, *J. Phys. Soc. Jpn.* **66**, 778 (1997).
- ²M. Reehuis, A. Krimmel, N. Büttgen, A. Loidl, and A. Prokofiev, *Eur. Phys. J. B* **35**, 311 (2003).
- ³S.-H. Lee, D. Louca, H. Ueda, S. Park, T. J. Sato, M. Isobe, Y. Ueda, S. Rosenkranz, P. Zschack, J. Íñiguez, Y. Qiu, and R. Osborn, *Phys. Rev. Lett.* **93**, 156407 (2004).
- ⁴M. Isobe and Y. Ueda, *J. Phys. Soc. Jpn.* **71**, 1848 (2002).
- ⁵M. Schmidt, W. Ratcliff II, P. G. Radaeli, K. Refson, N. M. Harrison, and S. W. Cheong, *Phys. Rev. Lett.* **92**, 056402 (2004).
- ⁶H. Tsunetsugu and Y. Motome, *Phys. Rev. B* **68**, 060405(R) (2003).
- ⁷O. Tchernyshyov, *Phys. Rev. Lett.* **93**, 157206 (2004).
- ⁸D. I. Khomskii and T. Mizokawa, *Phys. Rev. Lett.* **94**, 156402 (2005).
- ⁹K. I. Kugel and D. I. Khomskii, *Zh. Eksp. Teor. Fiz.* **64**, 369 (1973) [*Sov. Phys. JETP* **37**, 725 (1973)].
- ¹⁰K. Adachi, T. Suzuki, K. Kato, K. Osaka, M. Takata, and T. Katsufuji, *Phys. Rev. Lett.* **95**, 197202 (2005).
- ¹¹R. Plumier and M. Sougi, *Solid State Commun.* **64**, 53 (1987).
- ¹²R. Plumier and M. Sougi, *Physica B* **155**, 315 (1989).
- ¹³E. Nishibori, M. Takata, K. Kato, M. Sakata, Y. Kubota, S. Aoyagi, Y. Kuroiwa, M. Yamakata, and N. Ikeda, *Nucl. Instrum. Methods Phys. Res. A* **467-468**, 1045 (2001).
- ¹⁴W. Sugimoto, H. Yamamoto, Y. Sugahara, and K. Kuroda, *J. Phys. Chem. Solids* **59**, 83 (1998).
- ¹⁵C. Eylem, Y.-C. Hung, H. L. Ju, J. Y. Kim, D. C. Green, T. Vogt, J. A. Hriljac, B. W. Eichhorn, R. L. Greene, and L. Salamanca-Riba, *Chem. Mater.* **8**, 418 (1996).
- ¹⁶Y. Onose, N. Takeshita, C. Terakura, H. Takagi, and Y. Tokura, *Phys. Rev. B* **72**, 224431 (2005).